




Assessing excess mortality and heat-attributable risk during the summer of 2022 in Catalonia, Spain: a Bayesian spatiotemporal analysis

MariaA. Barceló^{1,2} · Marc Saez^{1,2} 

Received: 29 September 2024 / Accepted: 25 August 2025
© The Author(s) 2025

Abstract

In 2022, excess mortality in Spain was the third highest on record, surpassed only by 2020 and 2015. However, of that excess only 23% has been directly attributed to extreme heat. The problem with this figure is that the estimate is based on models that could present biases and limitations. We proposed to estimate the excess mortality attributable to extreme temperatures in Catalonia during the summer of 2022, and assessing how the risk of death from these extreme heat temperatures may be modified by other factors, particularly socioeconomic variables. We employed a longitudinal ecological design covering the period from 2015 to 2022, using data at the health area level. We used generalized linear mixed models for all ages and for those aged 65 and older. These models corrected for biases by using small-scale geographic units and explicitly took spatial variability into account. According to our results, during the summer months of 2022, 49.41% of excess mortality was attributable to extreme heat. Not only did heatwaves increase the risk of death, but so too did maximum temperature extremes. Effect modifiers found to increase the risk of dying on days with extreme heat were namely: being 65 years or older, high relative humidity, extreme minimum temperature, and low income. Our results suggest the following methodological considerations: (i) minimize the effects of exposure misclassification by using smaller geographic units than those typically used in other studies; (ii) explicitly take spatial variability into account by using, for example, a hierarchical Bayesian spatiotemporal models; and (iii) control for spatial and temporal dependencies.

Keywords Excess deaths · Heatwaves · Socioeconomic inequalities · Measurement errors · Bayesian spatiotemporal model

✉ Marc Saez
marc.saez@udg.edu

¹ Research Group on Statistics, Econometrics and Health (GRECS), University of Girona, Carrer de la Universitat de Girona 10, Campus de Montilivi, 17003 Girona, Spain

² Centro de Investigación Biomédica en Red de Epidemiología y Salud Pública, Instituto de Salud Carlos III, Madrid, Spain

1 Introduction

1.1 Summer 2022

During 2022, there was an excess of mortality throughout the world, in many cases only exceeded by the excess resulting from the COVID-19 pandemic in 2020. According to the European Mortality Monitoring system (EuroMOMO [2024](#)), between July 11 and August 14, 2022, Spain had an extraordinarily high excess mortality, with a particularly relevant contribution of deaths coming from the population aged 75 and over. Other countries, such as France, Germany (Hesse), Italy, and England, also showed a high excess of mortality, but not to the extent as Spain (EuroMOMO [2024](#)).

Official national mortality statistics are provided weekly from the 27 European countries or subnational regions in the EuroMOMO collaborative network, of which the (Spanish) ‘All-Cause Daily Mortality Monitoring System (MoMo)’ of the *Instituto de Salud Carlos III* is a partner.

According to the *Instituto de Salud Carlos III*’s data from its daily mortality surveillance system (MoMo [2024](#)), in 2022 excess mortality in Spain resulted in 30,479 deaths. In other words, the third highest since MoMo had come into effect and only surpassed by the 73,222 deaths in 2020 and the 38,523 in 2015. Furthermore, 2022 numbers were even greater than the 29,310 deaths in 2021 (the second year of the COVID-19 pandemic). In Catalonia, with 3567 deaths, 2022 was the fourth highest year of excess mortality (surpassed by 2020 (13,838 deaths), 2015 (4486 deaths), and 2021 (3655 deaths)) (Panel MoMo, [2024](#)). In the summer (June to August) of 2022, Spain presented the second highest mortality excess (20,291 deaths), surpassed only by 2003 (26,303 deaths) and 2015 (13,124 deaths). In Catalonia, during the summer months of 2022 excess mortality was 2290, which surpasses 2015 with its 1150 deaths (León et al. [2021](#); MoMo, [2024](#)).

During the summer of 2022, Spain accumulated 41 days of extreme temperatures via three heatwaves. In other words, beating the previous records established in 2015 (with two heatwaves) by 12 days, and in 2003 (also with two heatwaves) by 21 days. The July 2022 heatwave affected 44 of Spain’s 52 provinces, surpassing any previous record for the number of provinces affected by a heatwave. Furthermore, it exceeded the heatwaves of 2003, the year that had previously held the record with 38 provinces affected and presented a greater temperature anomaly (3.7 °C higher than the average for the month). Besides this, the first heatwave of 2022 (between June 12 and 18) was the second earliest on record, while the second heatwave between July 30 and August 15 was the most extensive and intense of those recorded until then (*Agencia Española de Meteorología -AEMET-*, 2024). Catalonia experienced its hottest summer since records began, surpassing 2003 in some areas. In Catalonia, with more than two weeks of temperatures above the usual average, the 2022 July heatwave was one of the most persistent (Meteocat [2022](#)).

It is surprising, therefore, that MoMo attributed slightly less than a quarter of the excess mortality directly to extreme heat during the summer months (only 4651 deaths or 22.92% in Spain, and 371 deaths or 16.22% in Catalonia). The problem lies in the estimates of excess mortality attributed to extreme heat provided by MoMo having been obtained from a model that may present limitations and biases.

In fact, even MoMo officials themselves acknowledged that they had probably underestimated the effects of the temperatures (Linde 2022). In this sense, Tobías et al. (2023a) using the same MoMo data but redefining extreme heat, estimated that actual heat-attributable deaths were two and a half times higher than the official estimates: 12,054 deaths—6738 in moderately high temperatures and 5316 in extreme temperatures; 60% of which occurred in the month of July. Using weekly counts of all-cause mortality according to sex and age groups from 823 contiguous regions in 35 European countries, Ballester et al. (2023), obtained the estimate for Spain from Eurostat and excess mortality attributed to extreme heat was equal to 11,324 (95% CI 7908, 14,880); a figure very close to that of Tobías et al. (2023a).

Among the principal limitations of the MoMo model, we firstly point out the use of the province as a geographical unit. Spain is administratively divided into 52 provinces, each with an average area of 9731 km² (standard deviation 5102 km², median 9316 km², first quartile 6205 km², third quartile 13,565 km²). Most importantly, it is assumed that all residents in the province were exposed to the same temperature values, i.e. exposure misclassification occurs. If the explanatory variables are measured inaccurately, as in this case, the estimators will be inconsistent (i.e. biased), tending to underestimate the effect of the variable measured with error (Greene 2018). Furthermore, if the between-area variability of the variables measured with error (temperature) is lower than the within-area variability, the effect of measurement error on the estimator can be considerable (Elliott and Savitz 2008). Furthermore, the MoMo model does not consider, and therefore does not control for, spatial dependence (closer areas look more similar than more distant ones). This omission is a specification error that leads to biased estimators whose variances are wrong. Finally, the model did not control for socioeconomic variables. In the most economically depressed territories, there might be a greater excess of mortality that can be attributed to extreme heat than in others.

Our hypothesis was that the limitations of the MoMo model implied a bias in the estimation of excess mortality. Thus, in this paper, we first attempt to estimate the excess mortality attributed to extreme heat temperatures in Catalonia in the summer of 2022 by using much smaller units of analysis, and temperature predictions obtained from a spatiotemporal Bayesian model, trying to solve the limitations of MoMo. In addition, we aim to assess how the risk of dying from these extreme heat temperatures may be modified by other factors, particularly socioeconomic variables.

1.2 Review of the literature

The literature on the effects of extreme heat, in general, and heatwaves, in particular, on mortality and, to a lesser extent, morbidity predates 2022. Indeed, although the

summer of 2022 broke temperature records across Europe, surprisingly few studies quantify the impact of extreme heat on mortality, and their findings are not entirely consistent.

Heatwaves are becoming one of the biggest climate-related threats to human health, as they've become more frequent, intense, and longer due to climate change (World Health Organization 2025). This global increase in extreme heat events is mainly linked to rising temperatures caused by climate change (EPA 2025). For instance, the USA saw record numbers of heat-related deaths in 2021 and 2022, which were also some of the hottest years on record. In India, the situation is just as worrying, especially in large urban areas where high population density increases the risk.

Heatwaves can affect health both directly and indirectly. The direct effects include things like heatstroke and dehydration. The indirect effects are often more serious and involve worsening existing conditions like heart and lung diseases (Ebi et al. 2021). Studies have shown that the risk of death goes up with more intense or longer heatwaves, especially those that come early in the summer, when people aren't yet used to the heat (World Health Organization 2025). Heat stress also impacts different body systems, with effects on heart and lung function, kidney health, and mental well-being (Arsad et al. 2022).

Plenty of research shows a strong link between heatwaves and higher mortality. For example, some studies found that deaths go up by 28% during heatwaves (95% CI 15–42%) (Cheng et al. 2018), while others reported an 11.6% increase in risk (95% CI 7.8–15.5%) (Kang et al. 2020). There is also evidence of more deaths from non-external causes, with relative risks between 1.03 and 1.09 (Arsad et al. 2022). Not all causes of death are affected equally—cardiovascular deaths seem especially sensitive, with a relative risk of 1.07 (95% CI 1.03–1.10). People with pre-existing breathing problems are also particularly at risk.

But these effects aren't the same for everyone. Older people, children, and those with chronic illnesses are especially vulnerable (World Health Organization 2025). In fact, around 85% of heat-related deaths happen in people over 65. This group is more likely to have heart conditions, and the risk of dying during a heatwave goes up by 12.8% (95% CI 9.8–15.9%) (Wang et al. 2015; Zhang et al. 2018; Arsad et al. 2022). Women are also more at risk than men, with studies showing higher relative risks in female populations (Yin et al. 2018; Kollanus et al. 2021). Socioeconomic status also matters a lot—people with lower incomes are more vulnerable, especially in cities where the urban heat island effect makes things worse (Nazish et al. 2024).

As for the summer of 2022, in Europe alone, it is estimated that there were 61,672 heat-related deaths, which shows just how serious the situation was (Ballester et al. 2023). These numbers were likely made worse by the urban heat island effect, which pushes city temperatures even higher. In California, a heatwave in September 2022 also led to a sharp rise in deaths, highlighting how urgently we need better heat protection measures (EPA 2025). Still, despite these extreme events, few studies have really measured how deadly heatwaves are, and the ones that do often show mixed results.

For example, Tobias et al. (2023a) said that the number of deaths in Europe during the 2022 heatwaves was similar to those during the deadly 2003 event. But their

study used national averages based on capital city temperatures and country-level death counts, which hides a lot of local detail. Similarly, Ballester et al. (2023) reported the same number of deaths (61,672), and again Spain was one of the hardest-hit countries. But without more local data, we do not know exactly where or among which groups the risks were highest.

Freitas et al. (2022) looked at Catalonia and found that the highest excess mortality in 2022 happened in rural areas and poorer neighbourhoods in cities. Older people and hospitalized patients were most affected. But the study didn't model the temperature-mortality link directly, so it is hard to say how much of the effect was due to heat itself. This is a wider problem. While earlier studies (like Gasparrini et al. 2022) show clear socioeconomic differences in heat risk, the data for 2022 is mostly anecdotal or indirect.

More recently, Quijal-Zamorano et al. (2024) looked at short-term links between temperature and deaths at the neighbourhood level in Barcelona. Their model accounted for spatial differences across the city's 73 neighbourhoods. However, they presented the analysis as a case study and did not give specific numbers for heat-related mortality, which limits its usefulness.

Another gap in the literature is the focus on officially defined heatwaves. Many studies ignore very hot days that don't meet the official threshold but are still dangerous. Tobias et al. (2023a), for example, found that moderately hot days actually caused more excess deaths (6738) than the officially defined.

2 Methods

2.1 Design

We used a time-series ecological design, from 2015 to 2022, with information on daily mortality, maximum temperature, and other meteorological variables (minimum temperature and relative humidity), as well as information on the average net income per person. All the variables were analysed at the (contextual) level of 288 health areas (ABS is the acronym in Catalan: *Àrea Bàsica de Salut*) that are managed by the public health service and distributed throughout the four provinces of Catalonia, Spain. We used a sample that covered 6.3 million people, accounting for 81.6% of the population of Catalonia and 76% of the ABSs into which Catalonia is divided.

2.2 Data sources

Daily deaths from all causes for all ages and 65 years and older were obtained from the Information System for the Development of Research in Primary Care (SIDIP in Catalan) (Recalde et al. 2022). The data were observed at an ecological level for each ABS.

We obtained information on the semi-hourly levels of the meteorological variables (maximum and minimum temperatures and relative humidity) for 2015–2022

from the 180 automatic meteorological stations in the Network of Automatic Meteorological Stations (XEMA in Catalan), excluding 12 meteorological stations that are at an altitude of 1500 m or more and which were active in the period (open data) (*Departament d'Acció Climàtica, Alimentació i Agenda Rural*, 2024). We averaged the semi-hourly data to obtain the daily data.

The average net incomes per person from 2015 to 2019 were obtained from the Spanish National Statistics Institute (INE in Spanish) (INE 2024a). This variable was observed at the census tract level. Using the population of each of the census tracts as weights (INE 2024b was the source of the total population of the census tract and of the population of the census tract by age and sex), we calculated the weighted average of the values at the census tracts that composed the ABS to obtain their value at ABS level. Finally, for each ABS we calculated the average from 2015 to 2019.

2.3 Excess mortality attributed to extreme temperatures

2.3.1 The MoMo model

Using data corresponding to the 288 ABSs in Catalonia for the period 2015–2022, we first applied the model used by the MoMo to predict excess all-cause mortality attributable to heat extremes in those ABSs.

$$\log(\theta_{it}) = \beta_0 + \beta_{1i} \text{ATO}_{it}^* + \text{spline}(\text{trend}_i, 1) + \text{spline}(\text{cyclic}_i, 6) + \text{offset}(\log(\text{Population}_i)) \quad (1)$$

where the subindexes i and t indicate the province and the day, respectively; θ_{it} is the mathematical expectation of Y_{it} , $E(Y_{it}) = \theta_{it}$ (i.e. the conditional risk of dying in province i on day t); and β_s are the coefficients of the explanatory and control variables. (e^β is the relative risk associated with each of them.)

The independent variables used to fit the model were: (i) trend, modelled as a rigid cubic spline (of order 1) by province; (ii) a cyclic spline (of order 6), to collect the annual seasonality of mortality, likewise by province; and (iii) the accumulated thermal overcharge variable (ATO^*) measuring the effect of maximum temperature, as a randomized effect between provinces, using mixed models (Díaz-Jiménez et al. 2015a). The ATO is a synthetic variable that measures the excess of temperature above a trigger temperature. The trigger thresholds for mortality due to excess maximum temperature assigned to each province a maximum critical temperature from which an increase in mortality was observed (Díaz-Jiménez et al. 2015b).

The ATO^* was calculated as (Díaz-Jiménez et al. 2015a):

$$\text{ATO}_i^* = \sqrt{\text{ATO}_{i-1} + \text{ATO}_{i-2} * 0.8 + \text{ATO}_{i-3} * 0.8^2 + \text{ATO}_{i-4} * 0.8^3 + \text{ATO}_{i-5} * 0.8^4 + \text{ATO}_{i-6} * 0.8^5 + \text{ATO}_{i-7} * 0.8^6}$$

where for each province i , $\text{ATO}_{i,t-k} = \text{Maximum temperature}_{i,t-1} - \text{Trigger temperature}_i$ ($k = 1, 2, \dots, 7$).

In the model, the death rate was adjusted, including the population of each age group, sex, and province (Population_i) as an offset (Díaz-Jiménez et al. 2015a).

Deaths attributable to excess in temperature were calculated as follows: (i) the model was adjusted with the independent variables of time and temperature (i.e. ATO*), thus obtaining the estimate of expected deaths with the effect of time and temperature; (ii) the model was adjusted with the independent time variables but without the temperature variables, thus obtaining the base estimate of expected deaths without the effect of temperature; and (iii) the difference between both estimates results in deaths attributable to excess of temperature (Díaz-Jiménez et al. 2015a).

2.3.2 Our model

Our hypothesis was that the limitations of the MoMo model introduce bias into the estimation of excess mortality attributable to extreme heat. Accordingly, our model was designed to address these limitations. There are six main differences between our model and that of the MoMo model. The two most important relate to sources of bias which, if not corrected, would likely underestimate the effects of high maximum temperature on mortality.

First, we used a much smaller geographic unit than the province: the ABS. Thus, while Catalonia is composed of four provinces, it is divided into 379 ABSs (of which we have information for 288). Of course, we were not free from exposure misclassification. However, if the within-area exposure variability is minimized and the between-area exposure variability is maximized, the effect of measurement error on the estimator consistency may be negligible (Elliott and Savitz 2008). As can be seen in Table S1 in the Supplementary material, by using ABSs we managed to minimize the within-area exposure variability and maximize the between-area exposure variability of the maximum temperature.

Second, the MoMo model considered that the temperature to which each subject is exposed is the average of the observed temperatures at the meteorological stations in the province. However, when there is a spatial variation in the study region, that is, in this case, between the different meteorological stations within the province, the use of the average can lead to bias and the underestimation of the health effect of interest (Wannemuehler et al. 2009). Furthermore, when the exposure is considered a representation of the average level of the true exposure across a population, we incur the so-called Berkson bias, also affecting the precision of the estimates. In our model, instead of using the observed temperature values at the meteorological stations of the ABS (40% of which did not have any meteorological stations), we used instead a hierarchical Bayesian spatiotemporal model which explicitly took this spatial variability into account, to make spatiotemporal predictions of the maximum and minimum temperature values as well as the relative humidity in each one of the ABSs. This approach gave us unbiased estimators with correct variances. (Details can be found in Saez and Barceló (2022)).

Third, trigger temperatures in the MoMo model were estimated for each province from the relationship between mortality and maximum temperature thus obtaining a single value for each province, whereas we considered the 95th percentile of the frequency distribution of the daily values of the spatiotemporal prediction of the maximum temperature in the period 2016–2021 (excluding the very possible outliers of

2015 and 2022) for each of the ABSs and each of the summer months (i.e. June, July, August, and September) as the trigger temperature. The choice of the 95th percentile was based on the definition from Spanish Ministry of Health's National Plan for Preventive Actions Against the Effects of Excess Temperatures on Health (Ministerio de Sanidad, Gobierno de España 2023; Tobías et al. 2023a) (see Table S2 in Supplementary material).

Fourth, in the MoMo model the coefficients associated with each lag of the ATO, although province-specific, were equal to 0.8^{k-1} , where k denotes lag. It is possible that the coefficients could vary not only by province, but also for each lag, in which case the estimators could be biased. We allowed the coefficients to be specific to each ABS and for each of the lags.

Fifth, the MoMo model did not control for spatial dependence. This omission led to biased estimators and wrong variances. We controlled for spatial dependence using a structured random effect (see below).

Finally, the MoMo model used a Poisson link. This link does not control for heteroscedasticity. In nonlinear models, this leads to biased estimators and wrong variances. Since the dependent variables were counting variables, the feasible approaches within the GLMM's family were the Poisson and negative binomial regression models. To allow for overdispersion, that is, when the actual variance is greater than the theoretical variance, or, in other words, to control for heteroskedasticity, we used negative binomial links. Furthermore, since many ABSs did not report any deaths on many days, we used zero-inflated counterpart links. Among the possibilities offered by the Integrated Nested Approximation (INLA) (Rue et al. 2009 and 2017), the best fit (understood as the link with the lowest WAIC [10]) was achieved with a zero-inflated negative binomial type 1. The log likelihood of this link was as follows:

$$\text{Prob}(y_i | \dots) = \text{weight}_i 1_{[y=0]} + (1 - \text{weight}_i) \times \text{Negative Binomial}(y_i)$$

where weight_i denotes the probability that in a specific ABS i , and on a given day t , there was at least one death.

Furthermore, albeit a difference that had no impact on the properties of the estimators is while in the MoMo model the trend and the annual seasonality were modelled as a rigid and cyclic cubic spline of orders 1 and 6, respectively, both by province, in our model we controlled for annual trend and seasonality using structured random effects, equivalent to smoothers (see below).

In particular, we used the following generalized linear mixed model (GLMM):

$$\log(\theta_{it}) = \beta_0 + \sum_{k=1}^7 \beta_{1i,k} \text{ATO}_{i,t-k} + \eta_i + S(\text{ABS}_i) + \tau_{it} + \tau_{s_{it}} + \text{offset}(\log(\text{Population}_i)) \quad (2)$$

where in this case, the subindexes i and t indicate the ABS, and the day, respectively; θ_{it} is the conditional risk of dying in ABS i on day t ; Population_i is the population at risk of being a case (death) in ABS i and on day t (i.e. the population of the ABS); and $\eta_i, S, \tau_{it}, \tau_{s_{it}}$ denote random effects.

We included four random effects in the models. First, η_i , a random effect indexed on ABS. This was unstructured (independent and identically distributed random effects), and captured individual heterogeneity, that is to say, unobserved confounders specific to the small area and invariant in time.

Second, in the model we included τ_{it} , a structured random effect (random walk of order one) indexed on time trend ($t=1,2,\dots,2783$) and specific to each ABS, to control the temporal dependency. Following the integrated nested Laplace approximations (INLA) approach (Rue et al. 2009 and 2017) when, as in our case, the random effects are indexed on a continuous variable, they can be used as smoothers to model nonlinear dependency on covariates in the linear predictor. Among the different smoothers available (i.e. autoregressive of order one, random walk of order one and random walk of order two), we chose the random walk of order 1 because, in addition to obtaining a moderate smoothing, it provided the highest predictive accuracy, measured by the Watanabe–Akaike information criterion (WAIC) (Watanabe 2010).

We also included τ_{its} , a structured random effect (cyclic random walk of order 2) indexed on month ($t=\text{June, July, August, September}$) and also specific to each ABS, in order to control seasonality.

Finally, we included the structured random effect, $S(\text{small area})$, to control spatial dependency. That is to say, the fact is that small areas that are close in space show more similar mortality than areas that are not close.

The spatially structured random effect S was normally distributed with zero mean and a Matérn covariance function:

$$\text{Cov}(S(x_i), S(x_{i'})) = \frac{\sigma^2}{2^{\nu-1}\Gamma(\nu)} (\kappa x_i - x_{i'})^\nu K_\nu(\kappa x_i - x_{i'})$$

where K_ν is the modified Bessel function of the second type and order $\nu > 0$. ν is a smoother parameter, σ^2 is the variance, and $\kappa > 0$ is related to the range ($\rho = \sqrt{8\nu/\kappa}$), the distance to which the spatial correlation is close to 0.1 (Lindgren et al. 2011).

2.4 Assessing the risk of dying from extreme temperatures

To accomplish our second objective, to assess how the risk of dying from these extreme heat temperatures may be modified by other variables, particularly socioeconomic variables, we estimated two GLMMs, one for maximum temperature extremes and the other for heatwaves, both stratified for all ages and 65 years and older:

$$\begin{aligned} \log(\theta_{it}') = & \gamma_0 + cb_i(\text{Extreme heat}_{i,t-k}) + \sum_{k=2}^4 \gamma_{2k,i} Q\text{Income}_{k,i} \\ & + cb_i(\text{maximum temperature}_{k,i}) \\ & + \eta_i + S(ABS_i) + \tau_{it} + \tau_{its} + \text{offset}(\log(\text{Population}_i)) \end{aligned} \quad (3)$$

where θ_{it}' is the conditional risk of a death (all ages and 65 years and older) in ABS i on day t , during the months June to September from 2015 to 2022; extreme heat

denotes an indicator of maximum temperature extreme or heatwave; $QIncome$ is an indicator of the quartile of average net income per person in which the ABS i is located (being the 4th quartile, i.e. the most economically favoured ABS, as the reference); maximum temperature is considered in ABS i on day t ; cb_i denotes two-dimensional function space that captures the dependency structure across both the predictor's domain and the lag dimension (i.e. cross-basis functions) (Gasparrini 2014); η_i is the unstructured random effect capturing individual heterogeneity; τ_{it} and τ_{its} are the structured random effects, capturing trend and annual seasonality; $S()$ is the structured random effects controlling spatial dependence (all of the random effects defined above); and Population denotes the population of the ABS i .

Note the subscript in the cross-basis functions and the coefficients, denoting that they were specified separately for each ABS.

In each of the ABSs, the maximum temperature extreme was defined as an indicator that the (spatiotemporal prediction of) maximum temperature exceeded the trigger temperature on a given day (1 extreme, 0 other case), while heatwave was an indicator that maximum temperature extremes occurred three or more days in a row at least 10% of the weather stations (*Ministerio de Sanidad, Gobierno de España, 2023*) (1 heatwave, 0 other case). As before, trigger temperature was defined as the 95th percentile of the frequency distribution of the daily values of the spatiotemporal prediction of the maximum temperature during the summer months in the period 2016–2021 in each one of the ABSs.

Cross-basis methods allowed us to use the distributed lag nonlinear models (DLNM) approach (Gasparrini et al. 2010; Gasparrini et al. 2011; Gasparrini 2014; Gasparrini et al. 2016; Gasparrini et al. 2022; Mistry and Gasparrini 2024). DLNM methods allowed us to simultaneously model the effects both maximum and extreme temperatures (extreme maximum temperatures and heatwaves), as well as the lag structure of these variables, have on the risk of death (all ages and subjects aged 65 years and older). The lags of the maximum temperature (up to 5), of the maximum temperature extremes (lag 7), and of the heatwaves (lag 3) were those corresponding to the models {3} with the highest WAIC (see Table S3 in Supplementary material). To capture the nonlinearity of the effects of the predictors, we built basis matrices, using natural cubic splines (with two equally spaced knots) for maximum temperature, and defined intervals (strata) for indicator variables (extreme maximum temperature, heatwaves, high relative humidity—fourth quartile) (Gasparrini et al. 2011; Lowe et al. 2021). We also used the WAIC to select both the functional forms for constructing the basis matrices and the optimal placement of the knots.

We allowed interactions between extreme heat and: (i) minimum temperature extremes (defined in the same way as the maximum temperature extremes, but with spatiotemporal prediction of minimum temperature and trigger minimum temperature); (ii) high relative humidity (fourth quartile); and (iii) average net income per person (income hereinafter) quartiles. Furthermore, we allowed third-order interactions between extreme heat, extremes of minimum temperature, and high relative humidity and income quartiles.

Once the models {3} had been estimated, we calculated the total effects of the variables of interest (extreme maximum temperature and heatwave), γ , as the sum of the (statistically significant) effects of the occurrence of the variable throughout the

lag structure. By exponentiating the total effects, we obtained the relative risks, RR (of the main effects), $RR = e^{\gamma}$.

As regard the interactions, the risk of dying on a day with extreme maximum temperatures or a heatwave can be calculated by multiplying the relative risks of the main effect and the interaction. In the case of a first-order interaction, for example: $RR = e^{\gamma_{\text{main effect}} + \gamma_{\text{interaction}}} = e^{\gamma_{\text{main effect}}} e^{\gamma_{\text{interaction}}}$, while in the case of third-order interaction: $RR = e^{\gamma_{\text{main effect}}} e^{\gamma_{\text{1st order interaction}}} e^{\gamma_{\text{2nd order interaction}}}$.

As explained above, to control for heteroskedasticity and given that many ABSs did not report any deaths on many days, we used a zero-inflated negative binomial type 1 as the link.

In all cases, the inferences were made following a Bayesian perspective, using the experimental mode (van Niekerk et al. 2024) of the integrated nested Laplace approximation (INLA) approach (Rue et al. 2009 and 2017). We used priors that penalize complexity (called PC priors). These priors are robust in the sense that they do not impact the results (Simpson et al. 2017). To model the distributed lag nonlinear models, we use the DLNM package (version 2.4.0) (Gasparrini et al. 2011).

3 Results

In Table 1 and Fig. 1, we provide some descriptives of the meteorological variables. In Fig. 1, in addition to the fact that maximum temperatures were much higher in 2022 (perhaps except for September), the extent of the territories with the highest maximum temperatures was much greater in the summer of 2022 than in the summers of 2015–2021 (even September). Note especially these two behaviours in June 2022.

As we see in Table 1, five heatwaves occurred in 2022, while between 2009 and 2015 there were 1.5 median heatwaves each year (2016, 2018, and 2020 one wave; 2015, 2021, and 2019 two waves). July 2022 had twice as many heatwaves as any month of July from 2015 to 2021. The median duration of heatwaves in 2022 (except September) was almost twice as long as the heatwaves from 2015 to 2021. The average maximum temperature (according to the median) in the summer of 2022 (except September) was slightly more than 2 °C higher than those of the period 2015–2021. In June 2022, it was 3.3 °C higher than the June months from 2015 to 2021.

In relation to the period 2015–2021, in the summer of 2022 (except September): the average minimum temperature (median) was between 0.83 and 1.92 °C higher, while the mean average temperature (median) was between 1 and 2.2 °C higher than those of the period 2015–2021. In June 2022, it was 2 °C higher than the June months from 2015 to 2021. As for the average (median) relative humidity in the summer of 2022, this was between 2 and 3.6% (June, July, and September) and 5.4% (August), i.e. higher than the period 2015–2021. Furthermore, compared to the 2015–2021 period, during heatwaves, the maximum temperature was 2.7 °C higher in July, and relative humidity was 4.54% higher in August and, above all, 14.15% higher in September. It is also worth noting that in September 2022, the minimum temperature on extreme days (including heatwave days) was about 1 °C higher.

Table 1 Descriptive of meteorological variables. 288 basic health areas (ABs) in Catalonia, Spain, managed by public health services

	June		July		August		September	
	2015–2021	2022	2015–2021	2022	2015–2021	2022	2015–2021	2022
Maximum Temperature (°C)	25.700 (6.370) 27.000 [23.30029.841]	30.392 (4.128) 30.300 [28.30032.784]	28.197 (7.044) 30.150 [26.90332.551]	32.566 (3.640) 32.800 [30.80034.800]	27.622 (6.890) 29.500 [26.10031.909]	31.578 (3.786) 31.830 [30.02233.794]	24.853 (5.704) 26.111 [24.30029.226]	26.440 (4.035) 26.600 [24.30029.226]
Extreme	35.552 (2.212) 36.470 [35.31238.093]	36.940 (1.855) 36.753 [35.50038.050]	36.697 (1.475) 37.327 [36.38438.312]	37.406 (1.961) 37.400 [36.44538.323]	37.676 (1.368) 37.593 [36.79238.506]	37.873 (1.406) 37.650 [37.00038.700]	33.914 (1.592) 33.724 [33.18235.200]	34.252 (1.590) 34.055 [33.18235.200]
Heatwave	37.462 (2.332) 36.950 [35.72539.000]	37.129 (1.866) 37.067 [35.72138.377]	37.896 (1.568) 35.190 [32.20037.285]	37.521 (1.328) 37.900 [36.80038.886]	38.056 (1.483) 37.912 [37.01039.900]	38.217 (1.450) 38.032 [37.24739.084]	34.300 (1.741) 34.200 [33.20035.306]	34.671 (1.662) 34.559 [33.51135.723]
Minimum Temperature (°C)	15.160 (3.383) 15.282 [12.85317.553]	17.016 (3.050) 17.200 [15.10719.153]	17.664 (3.074) 17.900 [15.72819.807]	19.034 (2.910) 19.300 [17.22121.013]	17.554 (3.205) 17.784 [15.46119.852]	18.386 (3.212) 18.618 [16.80120.625]	14.675 (3.582) 14.900 [12.20017.300]	14.972 (4.037) 15.100 [12.10018.004]
Extreme	18.000 18.221 (2.739)	18.400 18.551 (2.382)	18.988 19.021 (2.257)	19.356 19.248 (2.386)	20.167 20.102 (2.244)	20.257 20.739 (2.231)	17.812 18.135 (2.333)	19.000 19.148 (2.132)
Heatwave	18.192 [16.36420.005]	18.673 [17.066, 20.123]	18.981 [17.35020.552]	19.300 [17.54820.800]	20.291 [18.31721.794]	20.735 [19.30022.199]	18.133 [16.68019.800]	19.352 [17.83920.568]
Mean Temperature (°C)	20.834 (3.921) 21.265 [18.75723.520]	23.042 (3.445) 23.472 [21.49025.133]	23.533 (3.426) 24.185 [22.11025.727]	25.047 (3.204) 25.612 [23.94127.073]	23.040 (3.586) 23.646 [21.35925.331]	24.055 (3.499) 24.742 [22.67726.321]	19.624 (3.705) 20.127 [17.47922.290]	20.054 (3.862) 20.128 [17.73522.940]
Extreme	26.493 (3.818) 26.963 [25.54328.542]	26.489 (2.584) 26.836 [25.31228.166]	27.368 (2.011) 27.606 [26.60228.477]	27.382 (2.307) 27.817 [26.61128.749]	27.312 (2.550) 27.725 [26.38428.696]	27.538 (3.206) 28.160 [26.77129.219]	24.497 (2.931) 25.004 [23.65126.077]	24.895 (2.501) 25.316 [24.33226.016]
Heatwave	27.485 (2.215) 27.441 [26.18028.860]	27.709 (2.199) 27.668 [26.33429.242]	27.649 (1.977) 28.016 [26.84528.932]	28.047 (1.385) 28.068 [27.24028.975]	28.202 (2.305) 28.446 [27.41729.424]	28.594 (2.062) 28.756 [27.76529.827]	25.055 (2.145) 25.342 [24.15926.367]	25.589 (1.870) 25.736 [24.74826.764]

Table 1 (continued)

	June		July		August		September	
	2015–2021	2022	2015–2021	2022	2015–2021	2022	2015–2021	2022
Relative humidity, mean (%)	69.449 (14.194)	70.491 (15.576)	68.235 (13.794)	70.244 (16.390)	70.318 (13.235)	74.549 (13.540)	73.795 (11.970)	76.324 (11.839)
Extreme	67.860 [58.13781.757]	69.913 [57.72687.065]	65.798 [57.69178.732]	68.328 [55.91787.065]	68.951 [59.68680.866]	74.352 [63.65387.065]	74.272 [65.05482.639]	77.825 [67.70287.065]
Heatwave	56.339 (15.582)	59.180 (18.368)	59.154 (15.891)	60.109 (16.973)	60.893 (16.101)	65.960 (16.796)	66.436 (13.970)	74.384 (10.636)
	51.748	50.839	54.169	54.156	54.900	59.257	62.919	72.602
	[45.08359.681]	[44.72880.830]	[47.86563.201]	[47.38072.537]	[49.54868.117]	[52.63585.283]	[55.21875.987]	[66.57080.830]
	51.036 (11.292)	56.538 (17.498)	53.715 (13.064)	57.041 (15.988)	55.690 (13.866)	62.042 (15.864)	61.329 (13.329)	73.110 (9.182)
	48.353	49.083	50.536	51.473	51.716	56.251	57.381	71.531
	[43.81454.285]	[43.94063.288]	[45.17856.557]	[45.71660.084]	[47.45457.353]	[50.98369.350]	[52.57364.684]	[66.50480.259]
Number of heatwaves	1.000 (0.000)	1 heatwave	1.000 (0.000)	2 heatwaves	1 heatwave	1 heatwave	1 heatwave	1 heatwave
Heatwave duration (days)	1.000 [1.000.1.000]		1.000 [1.000.1.000]					
	4.670 (1.528)	8 days	5.000 (1.414)	5.500 (3.536)	4 days	6 days	6 days	3 days
	5.000 [3.000.5.000]		3.500 [3.000.5.500]	5.500 [3.000.5.500]				
Number of ABS affected by the heatwave	128 (80)	182 ABS	129 (16)	112 (51)	154 ABS	122 ABS	196 ABS	101 ABS
	107 [61.107]		126 [116.146]	112 [76.112]				
Date of the first heatwave	26 June 2015	8 June 2022	4 July 2015	9 July 2022		6 August 2022	8 September 2022	
							1 September 2016	
	26 June 2019		31 July 2018					
			22 July 2019					
			28 July 2020					
Maximum trigger temperature (°C)	10 June 2021				9 August 2021			
	34.742 (1.168)		36.012 (1.199)		36.591 (1.099)			

Table 1 (continued)

June		July		August		September	
2015–2021	2022	2015–2021	2022	2015–2021	2022	2015–2021	2022
34.754 [34.183,35.500]		36.067 [35.428,36.686]		36.605 [36.029,37.299]		32.698 [32.193,33.202]	

First row: mean (standard deviation). Second row: median [First quartile, Third quartile]
Spatiotemporal prediction of daily values of maximum, minimum temperature and relative humidity^[20]
(Maximum temperature) Extreme was defined as an indicator that the (the spatiotemporal prediction of the) maximum temperature exceeded the trigger temperature on a given day
Heatwave was an indicator that maximum temperature extremes occurred 3 or more days in a row in at least 10% of the weather stations
Trigger temperature was defined as the 95th percentile of the frequency distribution of the daily values of the spatiotemporal prediction of the maximum temperature during the summer months in the period 2016–2021 in each one of the ABSs

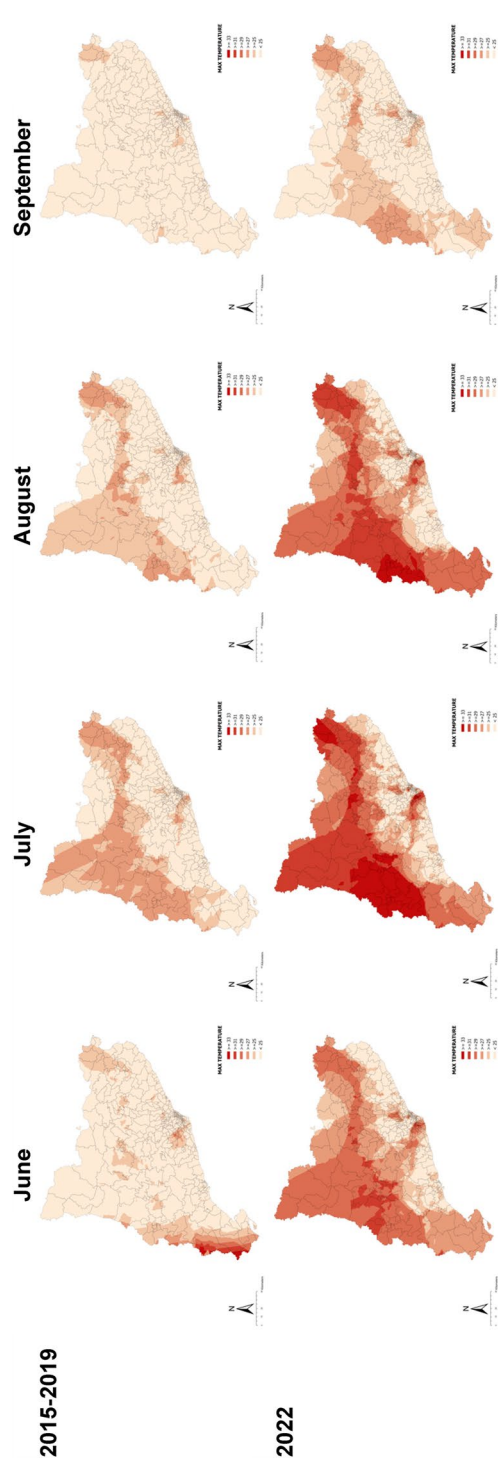


Fig. 1 Spatiotemporal prediction of the average daily maximum temperature during the summer months from 2015 to 2019 and 2022. Spatiotemporal prediction of daily values of maximum temperature^[20]

The estimates of excess mortality attributed to maximum temperature extremes are shown in Table 2. We estimated that, during the summer months of 2022, the excess mortality attributed to extreme heat was 49.41% (15.37% in MoMo). This excess is four times higher than that attributed to extreme heat in the summers of 2015 to 2019.

The results of the model estimation to assess the risk of dying from extreme maximum temperatures and heatwaves (main), as well as the first-order interactions (interactions), are shown in Figs. 2 and 3. We see that both heatwaves and extreme maximum temperature increased the risk of dying: 32.3% in the case of extreme maximum temperatures and 15.3% in the case of heatwaves. The risk of dying among individuals aged 65 years or older was similar for both extreme maximum temperatures and heatwaves, with estimated risks of 50.8% and 53.4%, respectively. This risk was almost double that of other subjects, especially in heatwaves. In both cases, all ages and 65 years or older, the effect of a heatwave on mortality occurs earlier (after 3 days) than with extreme maximum temperatures, which appeared after 7 days.

As regards first-order interactions, the risk of dying on a day with extreme temperatures (both maximum temperatures and heatwaves) and high relative humidity

Table 2 Estimation of excess mortality attributed to maximum temperature extremes according to the MoMo model and our model

Number of deaths	Observed		Excess deaths attributed to extreme heat	
	No COVID	COVID-19	MoMo model	Our model
2022				
June	4366	358	688	1854
July	5190	873	708	2779
August	4532	230	813	2241
September	4447	96	641	2284
June–September	18,535	1557	2850	9158
Medians				
2015–2019				
June	3235		334	577
July	3214		359	652
August	3375		263	651
September	3417		298	681
June–September	13,241		1254	2561
2020–2021				
June	3615	144	28	181
July	3841	224	43	274
August	4389	657	43	302
September	4004	309	17	303
June–September	16,248	267	131	1060

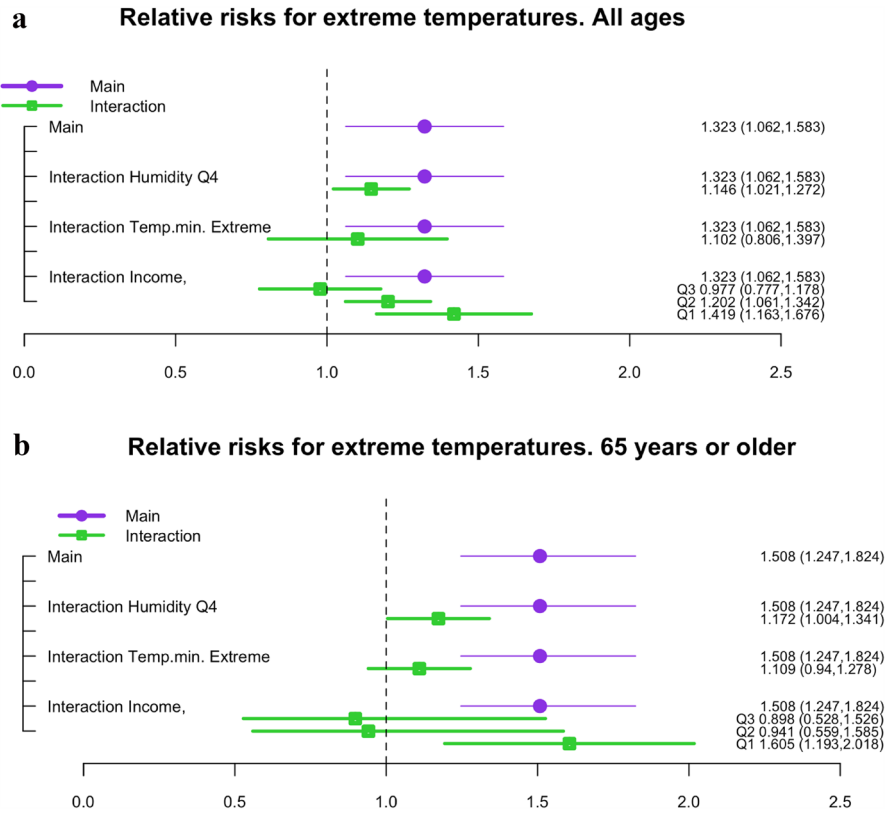


Fig. 2 **a** Results of the model estimation to assess the risk of dying from extreme temperatures, as well as the first-order interactions. Models adjusted for maximum temperature, average net income per person from the ABS, as well as individual heterogeneity; trend and annual seasonality; and spatial dependence. Population was included as offset. **b** Results of the model estimation to assess the risk of dying from extreme temperatures, as well as the first-order interactions. Models adjusted for maximum temperature, average net income per person from the ABS, as well as individual heterogeneity; trend and annual seasonality; and spatial dependence. Population was included as offset

(fourth quartile) was much higher than a day with only extreme temperatures (60% higher, $RR_{\text{main+interaction}} = 1.516$ vs. $RR_{\text{extreme}} = 1.323$, in extreme maximum temperatures and 35% higher, $RR_{\text{main+interaction}} = 1.4078$ vs. $RR_{\text{heatwave}} = 1.153$, in heatwaves) (see Figs. 2a and 3a). In the case of the risk of dying for those aged 65 years or older, the risk was 50.98% higher in extreme maximum temperatures ($RR_{\text{main+interaction}} = 1.767$ vs. $RR_{\text{extreme}} = 1.508$) and 279% higher in heatwaves ($RR_{\text{main+interaction}} = 2.489$ vs. $RR_{\text{heatwave}} = 1.534$) (see Figs. 2b and 3b).

The risk of dying on a day with extreme temperatures was almost three times higher ($RR_{\text{main+interaction}} = 1.877$ vs. $RR_{\text{extreme}} = 1.323$) in the case of extreme maximum temperatures, and almost double ($RR = 1.2948_{\text{main+interaction}}$ vs. $RR_{\text{heatwave}} = 1.153$) in the case of heatwaves, in those ABSs located in the first quartile (i.e. the most economically disadvantaged), compared to that of the least

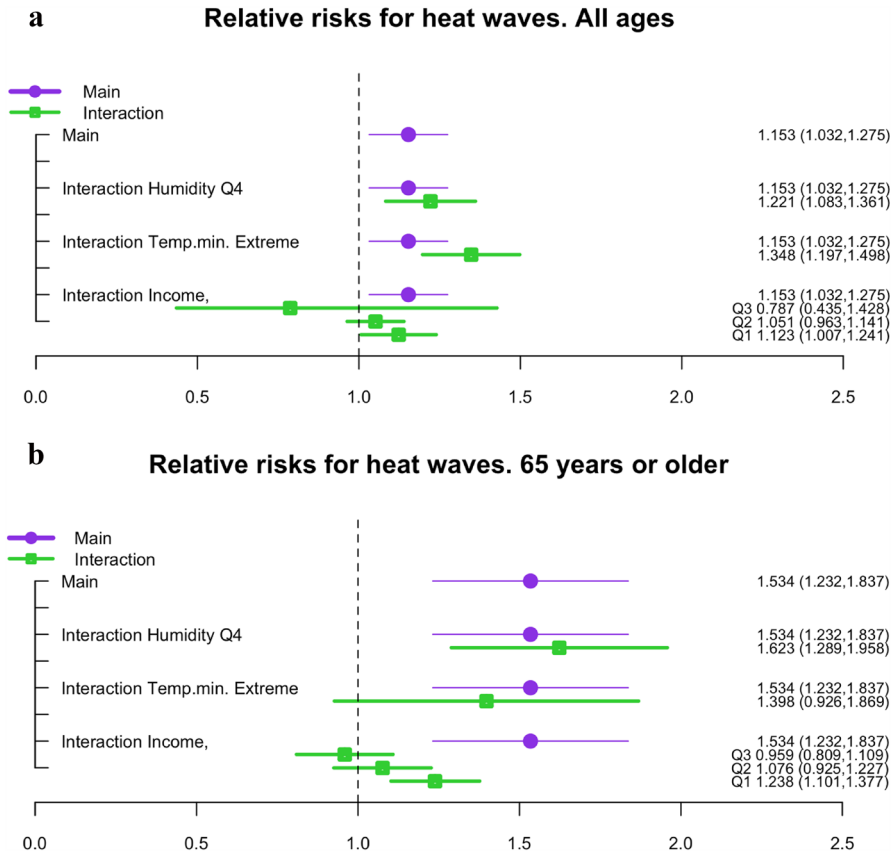


Fig. 3 **a** Results of the model estimation to assess the risk of dying from heatwaves, as well as the first-order interactions. Models adjusted for maximum temperature, average net income per person from the ABS, as well as individual heterogeneity; trend and annual seasonality; and spatial dependence. Population was included as offset. **b** Results of the model estimation to assess the risk of dying from heatwaves, as well as the first-order interactions. Models adjusted for maximum temperature, average net income per person from the ABS, as well as individual heterogeneity; trend and annual seasonality; and spatial dependence. Population was included as offset

economically disadvantaged ABSs (fourth quartile). In the case of subjects aged 65 years or older, the risk was practically triple in extreme maximum temperatures ($RR_{\text{main+interaction}} = 2.420$ vs. $RR_{\text{extreme}} = 1.508$) but 55.24% lower in heatwaves ($RR_{\text{main+interaction}} = 1.295$ vs. $RR_{\text{heatwave}} = 1.534$) (see Figs. 2b and 3b).

The risk of dying on a day with extreme maximum temperatures in ABSs located in the second income quartile was 82.7% higher than in those located in the first quartile (in the case of heatwaves in all ages and in all the cases in those subjects 65 years or older, the 95% credibility intervals contained unity, and therefore, they were not found to be statistically significant).

The interaction with extreme minimum temperatures was only statistically significant in the case of heatwaves and all ages. In a given ABS, on a heatwave day coinciding with an extreme minimum temperature, the risk of death was almost four times higher than on another day ($RR_{\text{main+interaction}} = 1.5542$ vs. $RR_{\text{heatwave}} = 1.153$).

Figure S1 in the Supplementary material shows the results of the estimation of the second-order interactions between heatwaves, minimum temperature extremes, and the average net income quartile of each ABS (in the remaining second-order interactions the 95% credibility intervals for these interactions contained 1 (i.e. they were not statistically significant). We see that the results described above were reproduced. On a heatwave day in which there was also an extreme minimum temperature in an ABS located in the second quartile of income, the RR of the main and both interaction effects was 2.44 ($RR_{\text{heatwave}} = 1.153$) for all ages and 36.73 ($RR_{\text{heatwave}} = 1.534$) for those subjects aged 65 years or more, i.e. 9.41 and 66.91 higher than those ABS located in the first quartile (i.e. the most disadvantaged).

4 Discussion

Using our model, we estimated that excess deaths attributed to extreme heat in the summer of 2022 in Catalonia were slightly more than three times those estimated using the MoMo model. This difference could be attributed to the effects of the biases incurred with the MoMo model. In particular, the exposure misclassification, a consequence of using the province as a geographic unit, and the bias caused by not considering the spatial variability within the geographical unit (i.e. simply averaging the maximum temperature observed at the meteorological stations in the province). As we mentioned, when left uncorrected both biases led to an underestimation of the effect of extreme temperatures on excess mortality.

Both Tobías et al. (2023a) and Ballester et al. (2023) estimated that actual heat-attributable deaths were two and a half times higher than the MoMo estimates. In addition to the fact that both provided estimates for the whole Spanish territory, there are some further differences with respect to our model.

Tobías et al. (2023b) did not analyse the months of September and only took into account mortality in provincial capitals. Although it is very likely that in their case, as in ours, the effect of exposure classification on the estimator consistency may have been negligible since, by using the provincial capitals, the within-area exposure variability would have been minimized, they did not, however, consider the spatial variability within the geographic unit by averaging the observed temperatures. This spatial variability could be particularly important in the city of Barcelona, with four meteorological stations separated by an average of 5 km (standard deviation 2 km, median 5.30 km, Q1 3.25 km, Q3 6.66 km) and with the stations at a mean altitude of 132.55 m (standard deviation 188.14 m, median 56 m, Q1 13.50 m, Q3 328.15 m). In Ballester et al. (2023), however, while they do not present the bias caused by ignoring the spatial variability of temperature within the geographic unit, since they used temperature data predicted in the high-resolution ERA5-Land reanalysis (European Centre for Medium-Range Weather Forecasts 2023) which takes into account such variability, it was not free from exposure misclassification.

Ballester et al. (2023) used the 59 NUTS 3 into which Spain is divided. In the case of Spain, NUTS 3 corresponds to the province and each one of the Canary and Balearic Islands. However, in the latter case, Ibiza and Formentera are grouped together and are considered three NUTS 3, instead of four like the actual number of islands (i.e. Mallorca, Menorca and Ibiza-Formentera). However, neither we nor Tobias et al. (2023a) nor Ballester et al. (2023) were free from Berkson bias, so the confidence intervals (credibility in our case) may have been wider than appropriate. It should be noted, however, that in Ballester et al. (2023), the 95% confidence interval estimator also tripled the official estimates, as in our case (Tobías et al. 2023a, did not provide the confidence interval).

As regards the analysis of the risk of dying, we found that it was not necessary for a heatwave to occur for the risk of dying to increase, it was enough for the maximum temperature to be extreme, that is, above the trigger temperatures (i.e. the 95th percentile of the distribution of maximum temperature during the summer months for each of the months and for each ABSs). On those days, the risk of dying increased in a range between 15% (in heatwaves) and 32% (in extreme maximum temperatures). In fact, along the same lines as our results, although using a different model with other objective, Tobias et al. (2023a and 2023b) found that excess deaths also occur with extreme heat and not only in heatwaves.

We estimated a lagged effect of maximum temperature extremes on mortality equal to one week, while that of heatwaves was three days. Tobías et al. (2023a), using the daily average temperature, also found lagged effects of up to a week.

We found effect modifiers of the risk of dying on a day with extreme heat (extreme maximum temperature and heatwave), both at the individual level: (being 65 years or older), and at the contextual (the ABS) level: high relative humidity, extreme minimum temperature, and low income (first and second quartiles). When an ABS was in the most economically disadvantaged area (first quartile) the risk of dying in the all ages case, tripled in extreme maximum temperatures days, and doubled, during heatwaves, and was three times higher in heatwaves, in subjects aged 65 years or older (in all cases compared to the fourth quartile, the least disadvantaged).

Since we found that the effect of maximum temperature extremes on mortality occurred earlier than that of heatwaves (7-day delay vs. 3-day delay, respectively), some harvesting effect may have occurred, with fewer subjects at risk of dying (i.e. more dying earlier) when heatwaves occurred. This would be reflected in, firstly, a lower risk (for all ages) in the case of heatwaves (1.323 in extreme maximum temperatures and 1.153 in heatwaves). Furthermore, this harvesting effect had more influence in subjects aged 65 years or older on very humid days (fourth quartile) and, above all, during heatwaves in subjects living in the most economically disadvantaged ABSs (compare $RR_{\text{main+interaction heatwave:Q1 income}} = 1.295$ vs. $RR_{\text{heatwave}} = 1.534$; with $RR_{\text{main+interaction extreme maximum temperature:Q1 income}} = 2.420$ vs. $RR_{\text{heatwave}} = 1.508$).

Again, using different approaches with different objectives, Ballester et al. (2023) and Freitas et al. (2022), for the summer of 2022, and Gasparrini et al. (2022), for the period 2000–2019, found that excess mortality attributed to extreme heat was higher in older population groups. Thus, Ballester et al. (2023), using data from 823 contiguous regions in 35 European countries, found higher heat-related mortality

rates in the age group 65 years or older, although the rates were higher in men than in women for the age group 65–79 years, but higher in women than in men for people aged 80+ years. For Catalonia, Freitas et al. (2022) point out an excess mortality in the summer of 2022, compared to the summer of 2019, for the age group 55 years or older, finding the maximum differences in the 80–84 age group in both sexes and over 90 years in women. Gasparrini et al. (2022), analysing 34,753 lower super output areas across England and Wales for 2000–2019, found that, compared to the under 65 age group, the 75 to 84 age groups and, above all, those 85 years and older, had a higher risk of death attributed to extreme heat.

As regards socioeconomic status, as we have noted, only Freitas et al. (2022) took socioeconomic status into account. They point out that in the rural areas and in the most socioeconomically depressed urban ABSs, the excess of deaths attributed to extreme heat was higher. However, the raw and standardized rates (by age and sex) were not significantly higher than those of the remaining areas.

5 Conclusions

Summing up, our analysis reveals that extreme heat during the summer of 2022 in Catalonia had a far greater mortality impact than previously estimated, with excess deaths three times higher than those derived from the MoMo model (49.41% vs. 15.37%). This underestimation likely arises from methodological biases, particularly exposure misclassification and spatial aggregation of temperature data, which obscure localized heat effects. Notably, mortality risk increased not only during heatwaves (15% higher risk) but also on days with isolated extreme temperatures (32% higher risk), with delayed effects lasting up to one week for extreme heat and three days for heatwaves. These lagged patterns suggest prolonged physiological stress from sustained heat exposure, even in the absence of formal heatwave conditions. Vulnerability was further exacerbated by individual and contextual factors: older adults (≥ 65 years), residents of low-income areas (where risk tripled during extreme heat), and populations exposed to high humidity or elevated night-time temperatures experienced disproportionately high impacts. Our findings underscore the need to move beyond heatwave-centric warnings and adopt more granular, spatially explicit risk assessments that account for both immediate and delayed heat effects, particularly in socioeconomically vulnerable communities.

Our study may have several limitations. First, the observational ecological design precludes individual-level inferences (to avoid ecological fallacy) and causal interpretations, while unmeasured biases inherent to such designs may persist. However, we addressed this by adjusting for observed confounders and incorporating unstructured and structured random effects, which captured unobserved spatial and temporal dependencies at the small-area level. Second, generalizability is constrained because: SIDIAP records only primary care-reported deaths, omitting 35.4% of hospital-recorded deaths in Catalonia (Freitas et al. 2022), and 24% of ABS areas (18.4% of the population) were excluded. These excluded areas, managed outside the public health service, cluster in warmer regions (e.g. southern Catalonia), potentially biasing estimates, though the direction of this bias remains indeterminate.

Third, while our 95th percentile trigger temperature aligns with the Spanish Ministry of Health's National Plan (2023) and prior work (Tobías et al., 2023a, 2023b), it reflects a meteorological rather than physiological threshold. Notably, our province-specific median thresholds were lower than MoMo's epidemiologically derived values (Supplementary Material, Table S2). Finally, exposure misclassification may arise as individuals' mobility (e.g. workplaces, holidays) means residential ABS temperatures may not reflect true exposure. However, this misclassification is likely non-differential, equally affecting all subjects.

These limitations can largely be offset by the strengths of our study. Firstly, we significantly reduced exposure misclassification by working with much smaller geographic units than typically used in comparable studies. Estimates at a smaller geographic level have only been carried out by Gasparrini et al. (2022), who analysed temperature-related mortality across 34,753 lower super output areas (LSOAs) in England and Wales, and Quijal-Zamorano et al. (2024), who conducted neighbourhood-level analyses for Barcelona's 73 districts. Secondly, our hierarchical Bayesian spatiotemporal model explicitly accounted for spatial variability, generating predictions of maximum temperature and other meteorological variables for each ABS. This approach prevented underestimation of extreme temperature effects on mortality. Finally, by incorporating spatial dependence controls—a methodological refinement rarely implemented in small-area analyses—we obtained more reliable estimators with appropriate variances. As demonstrated by Quijal-Zamorano et al. (2024), such spatial adjustments are crucial for producing stable, plausible estimates, particularly in areas with low mortality counts where conventional models often fail.

Regarding future research directions, we would like to expand our research along four main lines. First, we will expand both the population, i.e. from the 288 ABSs analysed (81.6% of the population and 76% of the ABSs in which the territory of Catalonia is divided) to the 379 ABSs (100% of the population and of the ABSs); and the time period, considering 2023 to 2024, years in which there could have been higher temperatures (average and maximum), a greater number of extreme episodes, and a greater effect on mortality than in 2022. Second, we will explore the interaction between extreme heat and exposure to air pollution during the summer months, considering both average and extreme pollution levels. Third, we will incorporate individual-level data, not only for mortality but also for morbidity, enabling us to control for both contextual and individual-level confounders such as sex, age, comorbidities, and individual income, among others. Finally, we plan to advance the modelling of the spatiotemporal dimension. Rather than treating space and time independently (as in our current approach), we will examine them as dependent but separable—as in Quijal-Zamorano et al. (2024)—and, importantly, as dependent and non-separable, allowing for more realistic and nuanced inference.

Climate change projections suggest increasing importance of our research, with rising global temperatures expected to increase frequency, intensity, duration, and severity of heat waves (Barriopedro et al. 2023; EPA 2025). This trend poses significant challenges for public health systems, which must adapt to the growing threat. Effective strategies include early warning systems, public education campaigns, and infrastructure improvements to reduce urban heat islands.

In conclusion, our results suggest that one should: (i) minimize the effects of exposure misclassification by using smaller geographic units than those used in other studies; (ii) explicitly took spatial variability into account, using for example a hierarchical Bayesian spatiotemporal model; and (iii) control for spatial and temporal dependencies.

Supplementary Information The online version contains supplementary material available at <https://doi.org/10.1007/s10109-025-00475-2>.

Acknowledgements This study was carried out within the ‘Collaboration agreement between Dipsalut and the University of Girona to promote and develop joint work in relation to health inequalities generated by the social determinants of health and environmental factors’, and within the ‘Health Inequalities and COVID-19’ and ‘Atlas of Social and Environmental Determinants of Health’ subprogrammes of CIBER of Epidemiology and Public Health (CIBERESP). A preliminary version of this paper was presented at the 22nd International Workshop in Spatial Econometrics and Statistics (SEW’2024), held in Grenoble, France, from May 23 to 25, 2024. We are grateful to two anonymous reviewers for their constructive comments on an earlier version of this work, which have undoubtedly helped us to improve it. The usual disclaimer applies.

Author contributions Both authors were responsible for conceptualization, methodology, resources, data curation, analysis, writing—original draft preparation, writing—review and editing, project administration, and funding acquisition.

Funding Open Access funding provided thanks to the CRUE-CSIC agreement with Springer Nature. This work was partially financed by AGAUR, the Department of Climate Action, Food and Rural Agenda and by the Department of Research and Universities, both from the Government of Catalonia (*Generalitat de Catalunya*) (grants number 2023 CLIMA 00037 and 2021 SGR 01197). The funding sources did not participate in the design or conduct of the study, the collection, management, analysis, or interpretation of the data, or the preparation, review, and approval of the manuscript.

Availability of data and materials Regarding the mortality data, although aggregated, due to ethical (in accordance with the protocol approved by the Ethics Committees of ‘Fundació Institut Universitari per a la Investigació en Atenció Primària de Salut Jordi Gol i Gurina -IDIAPJGol-’) and legal regulations (both the provisions of the Spanish Law 3/2018, of December 5, on Personal Data Protection and Guarantee of Digital Rights, such as the Collaboration Agreement for which the project SLT/3896/2021 is executed), there are restrictions on the transfer of data to third parties and data are not publicly available. However, after approval of the research proposal plan and with a signed data access agreement, and upon reasonable request to the corresponding author, data (properly anonymized) will be available. The rest of the data is open data: **Meteorological data:** Departament d’Acció Climàtica, Alimentació i Agenda Rural. Dades meteorològiques de la XEMA [in Catalan] [Available at: https://analisi.transparenciacatalunya.cat/ca/Medi-Ambient/Dades-meteorol-giques-de-la-XEMA/nzvn-apee/about_data, last accessed on August 28, 2024]. **Socioeconomic data:** INE. Instituto Nacional de Estadística. Household income distribution map [Available at: https://www.ine.es/dyngs/INEbase/en/operacion.htm?c=Estadistica_C&cid=1254736177088&menu=ultiDatos&idp=1254735976608, last accessed on August 28, 2024]. **Population data:** INE. Instituto Nacional de Estadística. Continuous Register Statistics. [Available at: https://www.ine.es/dyngs/INEbase/en/operacion.htm?c=Estadistica_C&cid=1254736177012&menu=ultiDatos&idp=1254734710990, last accessed on August 28, 2024]. The code will be available at www.researchprojects.es.

Declarations

Competing interest The manuscript is an original contribution that has not been published before, whole or in part, in any format, including electronically. All authors will disclose any actual or potential conflict of interest including any financial, personal, or other relationships with other people or organizations that could inappropriately influence or be perceived to influence their work, within three years of beginning the submitted work.

Generative AI and AI-assisted technologies in the writing process During the writing of the article, the authors have not used any type of AI or AI-assisted technologies.

Ethics approval and consent to participate All methods were carried out in accordance with relevant guidelines and regulations. Regarding mortality data, data usage from the Information System for Research in Primary Care (SIDIAP) is authorized by the Catalan Health Institute (ICS) and the Data Analysis Program for Health Research and Innovation (PADRIS). These public organizations ensure the protection of individuals' privacy through pseudo-anonymization of the data. For linking with other public data sources, ICS or PADRIS serves as Trusted Third Parties (TTPs) to perform the linkage process and provide the newly pseudo-anonymized dataset. In cases where access to personal data requires patient consent, the same TTPs are involved. SIDIAP does not provide re-identifiable information, implementing measures such as aggregations and deletions to maintain pseudo-anonymization. All data management adheres to legal requirements, including the General Data Protection Regulation (EU) 2016/679 and Organic Law 3/2018, of 5 December, which safeguards personal data and digital rights. Secure servers were used for data storage, ensuring compliance with these regulations. As patient data extracted from the database were irreversibly pseudonymized, written informed consent was not required.

Open Access This article is licensed under a Creative Commons Attribution 4.0 International License, which permits use, sharing, adaptation, distribution and reproduction in any medium or format, as long as you give appropriate credit to the original author(s) and the source, provide a link to the Creative Commons licence, and indicate if changes were made. The images or other third party material in this article are included in the article's Creative Commons licence, unless indicated otherwise in a credit line to the material. If material is not included in the article's Creative Commons licence and your intended use is not permitted by statutory regulation or exceeds the permitted use, you will need to obtain permission directly from the copyright holder. To view a copy of this licence, visit <http://creativecommons.org/licenses/by/4.0/>.

References

- Agencia Española de Meteorología (AEMET). Olas de calor en España desde 1975 [in Spanish] [Available at: https://www.aemet.es/es/conocermas/recursos_en_linea/publicaciones_y_estudios/estudios/detalles/olascalor. Accessed 2 June 2025]
- Arsad FS, Hod R, Ahmad N, Ismail R, Mohamed N, Baharom M, Osman Y, Mohd-Radi MF, Tangang F (2022) The impact of heatwaves on mortality and morbidity and the associated vulnerability factors: a systematic review. *Int J Environ Res Public Health* 19(23):16356. <https://doi.org/10.3390/ijerph192316356>
- Ballester J, Quijal-Zamorano M, Méndez Turrubiates RF, Pegenaute F, Herrmann FR, Robine JM, Basagaña X, Tonne C, Antó JM, Achebak H (2023) Heat-related mortality in Europe during the summer of 2022. *Nat Med* 29:1857–1866. <https://doi.org/10.1038/s41591-023-02419-z>
- Barriopedro D, García-Herrera R, Ordóñez C, Miralles DG, Salcedo-Sanz S (2023) Heat waves: physical understanding and scientific challenges. *Rev Geophys*. <https://doi.org/10.1029/2022RG000780>
- Cheng J, Xu Z, Bambrick H, Su H, Tong S, Hu W (2018) Heatwave and elderly mortality: an evaluation of death burden and health costs considering short-term mortality displacement. *Environ Int* 115:334–342. <https://doi.org/10.1016/j.envint.2018.03.041>
- Departament d'Acció Climàtica, Alimentació i Agenda Rural. Dades meteorològiques de la XEMA [in Catalan] [Available at: https://analisi.transparenciacatalunya.cat/ca/Medi-Ambient/Dades-meteoroliques-de-la-XEMA/nzvn-apee/about_data. Accessed 2 June 2025]
- Díaz-Jiménez J, Linares C, Carmona R. Temperaturas umbrales de disparo de la mortalidad atribuible al calor en España en el período 2000–2009. Escuela Nacional de Sanidad, Instituto de Salud Carlos III, Ministerio de Economía y Competitividad, 2015a [in Spanish] [Available at: <http://gesdoc.isciii.es/gesdoccontroller?action=download&id=24/07/2015-fe69310aba>. Accessed 28 Aug 2024]
- Díaz-Jiménez J, Carmona R, Linares C. Temperaturas umbrales de disparo de la mortalidad atribuible al calor en España en el período 2000–2009. Escuela Nacional de Sanidad, Instituto de Salud Carlos III, Ministerio de Economía y Competitividad, 2015b [in Spanish] [Available at: <http://gesdoc.isciii.es/gesdoccontroller?action=download&id=24/07/2015-fe69310aba>. Accessed 28 Aug 2024]

- Ebi KL, Vanos J, Baldwin JW, Bell JE, Hondula DM, Erret NA, Hayes K, Reid CE, Saha S, Spector H, Berry P (2021) Extreme weather and climate change: population health and health system implications. *Annu Rev Public Health* 42:293–315. <https://doi.org/10.1146/annurev-publhealth-012420-105026>
- Elliott P, Savitz DA (2008) Design issues in small-area studies of environment and health. *Environ Health Perspect* 116(8):1098–1104. <https://doi.org/10.1289/ehp.10817>
- EPA. United States Environmental Protection Agency. Climate Change Indicators. 2025 [Available at: <https://www.epa.gov/climate-indicators/climate-change-indicators-heat-waves>. Accessed 5 June 2025]
- EuroMOMO Bulletin [available at: <https://www.euromomo.eu/bulletins/2022-34>. Accessed 2 June 2025]
- European Centre for Medium-Range Weather Forecasts. ERA5-Land Hourly Data from 1950 to Present [Available at: <https://cds.climate.copernicus.eu/cdsapp#!/dataset/reanalysis-era5-land?tab=overview>. Accessed 2 June 2025]
- Freitas A, Langerita R, Molina P, Mompart A, Planella A, Plaza A, Sales J, Cabezas C, Mendioroz J, Coma E, Fina F, Medina M, Mora N, Coca M, Vela E, Pino D. L'excés de mortalitat a Catalunya. Anàlisi de l'excés de mortalitat de l'1 de juny al 31 d'agost de 2022. Generalitat de Catalunya, Departament de Salut, 2022 [in Catalan] [Available at: <https://salutweb.gencat.cat/ca/detalls/Noticies/noti-mortalitat>. Accessed 28 Aug 2024]
- Gasparrini A (2014) Modeling exposure-lag-response associations with distributed lag non-linear models. *Stat Med* 33(5):881–899. <https://doi.org/10.1002/sim.5963>
- Gasparrini A, Armstrong B, Kenward MG (2010) Distributed lag non-linear models. *Stat Med* 29(21):2224–2234. <https://doi.org/10.1002/sim.3940>
- Gasparrini A, Armstrong B, Scheipl F (2011) Distributed lag linear and non-linear models in R: the package dlnm. *J Stat Softw* 43(8):1–20. <https://doi.org/10.18637/jss.v043.i08>
- Gasparrini A, Guo Y, Hashizume M, Lavigne E, Tobias A, Zanobetti A, Schwartz J, Leone M, Michelozzi P, Haidong K, Tong S, Honda Y, Kim H, Armstrong BG (2016) Changes in susceptibility to heat during the summer: a multi-country analysis. *Am J Epidemiol* 183(11):1027–1036. <https://doi.org/10.1093/aje/kwv260>
- Gasparrini A, Masselot P, Scortichini M, Schneider R, Mistry MM, Sera F, Macintyre HL, Phalkey R, Vicedo-Cabrera AM (2022) Small-area assessment of temperature-related mortality risks in England and Wales: a case time series analysis. *Lancet Planet Health* 6(7):e557–e564. [https://doi.org/10.1016/S2542-5196\(22\)00138-3](https://doi.org/10.1016/S2542-5196(22)00138-3)
- Greene WH (2018) *Econometric analysis*, 8th edn. Pearson, Boston
- INE (2024a) Instituto Nacional de Estadística. Household income distribution map [Available at: https://www.ine.es/dyngs/INEbase/en/operacion.htm?c=Estadistica_C&cid=1254736177088&menu=ultiDatos&idp=1254735976608. Accessed 2 June 2025]
- INE (2024b) Instituto Nacional de Estadística. Continuous Register Statistics. [Available at: https://www.ine.es/dyngs/INEbase/en/operacion.htm?c=Estadistica_C&cid=1254736177012&menu=ultiDatos&idp=1254734710990. Accessed 2 June 2025]
- Kang C, Park C, Lee W, Pehlivan N, Choi M, Jang J, Kim H (2020) Heatwave-related mortality risk and the risk-based definition of heat wave in South Korea: a nationwide time-series study for 2011–2017. *Int J Environ Res Public Health* 17:5720. <https://doi.org/10.3390/ijerph17165720>
- Kollanus V, Tiittanen P, Lanki T (2021) Mortality risk related to heatwaves in Finland—factors affecting vulnerability. *Environ Res* 201:111503. <https://doi.org/10.1016/j.envres.2021.111503>
- León I, Frías L, Delgado C, Larrauri A. Informe MoMo. Estimaciones de la mortalidad atribuible a excesos de temperatura en España, 1 de junio a 15 de septiembre de 2021. Plan nacional de acciones preventivas contra los efectos del exceso de temperaturas sobre la salud. Centro Nacional de Epidemiología. Ciber de Epidemiología y Salud Pública (CIBERESP). Instituto de Salud Carlos III. Diciembre 2021 [in Spanish] [Available at: https://www.isciii.es/QueHacemos/Servicios/VigilanciaSaludPublicaRENAVE/EnfermedadesTransmisibles/MoMo/Documents/Informe_MoMocalor_verano2021.pdf. Accessed 28 Aug 2024]
- Linde P. Las olas de calor y la COVID (sobre todo) causaron 34.000 muertes más de las previstas en 2022 en España [in Spanish]. *El País*, January 8, 2023.
- Lindgren FK, Rue H, Lindström J (2011) An explicit link between Gaussian fields and Gaussian Markov random fields: the stochastic partial differential equation approach. *J R Stat Soc Series B Stat Methodol* 73(4):423–498. <https://doi.org/10.1111/j.1467-9868.2011.00777.x>

- Lowe R, Lee SA, O'Reilly KM, Brady OJ, Bastos L, Carrasco-Escobar G, de Castro CR, Colón-González F, Barcellos C, Sá Carvalho M, Blangiardo M, Rue H, Gasparrini A (2021) Combined effects of hydrometeorological hazards and urbanisation on dengue risk in Brazil: a spatiotemporal modelling study. *Lancet Planet Health* 5(4):e209–e219. [https://doi.org/10.1016/S2542-5196\(20\)30292-8](https://doi.org/10.1016/S2542-5196(20)30292-8)
- Meteocat. Balanç d'una de les onades de calor més persistents mesurades a Catalunya, juliol 2022 [in Catalan] [Available at: <https://govern.cat/salaprensa/notes-premsa/430602/balanc-d-una-de-les-onades-de-calor-mes-persistents-mesurades-a-catalunya>. Accessed 2 June 2025]
- Ministerio de Sanidad, Gobierno de España. Plan Nacional de actuaciones preventivas de los efectos del exceso de temperaturas sobre la salud 2023 [in Spanish] [Available at: https://www.sanidad.gob.es/ciudadanos/saludAmbLaboral/planAltasTemp/2023/docs/Plan_Excesos_Temperatura_2023.pdf. Accessed 28 Aug 2024]
- Mistry MN, Gasparrini A (2024) Real-time forecast of temperature-related excess mortality at small-area level: towards and operational framework. *Environ Res Health* 2(3):035011. <https://doi.org/10.1088/2752-5309/ad5f51>
- MoMo, ISCHII. MoMo. Monitorización de la mortalidad diaria por todas las causas y atribuible a temperatura. Situación a 30 de agosto de 2022 [in Spanish] [Available at: https://www.iscii.es/QueHacemos/Servicios/VigilanciaSaludPublicaRENAVE/EnfermedadesTransmisibles/MoMo/Documents/InformesMoMo2022/MoMo_Situación%20a%2030%20de%20agosto%20de%202022_CNE.pdf. Accessed 28 Aug 2024]
- Nazish A, Abbas K, Sattar E (2024) Health impact of urban green spaces: a systematic review of heat-related morbidity and mortality. *BMJ Open* 14(9):e081632. <https://doi.org/10.1136/bmjopen-2023-081632>
- Panel MoMo, ISCHII [Available at: https://momo.iscii.es/panel_momo/. Accessed 2 June 2025]
- Quijal-Zamorano M, Martínez-Beneito MA, Ballester J, Marí-DellOlmo M (2024) Spatial Bayesian distributed lag non-linear models (SB-DLNM) for small-area exposure-lag-response epidemiological modelling. *Int J Epidemiol* 53(3):dyae061. <https://doi.org/10.1093/ije/dyae061>
- Recalde M, Rodríguez C, Burn E, Far M, García D, Carrere-Molina J et al (2022) Data resource profile: The information system for research in primary care (SIDIAP). *Int J Epidemiol* 51:e324–e336. <https://doi.org/10.1093/ije/dyae068>
- Rue H, Martino S, Chopin N (2009) Approximate Bayesian inference for latent Gaussian models using integrated nested Laplace approximations (with discussion). *J R Stat Soc Ser B Stat Methodol* 71:319–392. <https://doi.org/10.1111/j.1467-9868.2008.00700.x>
- Rue H, Riebler A, Sørbye H, Illian JB, Simpson DP, Lindgren FK (2017) Bayesian computing with INLA: a review. *Annu Rev Stat Appl* 4(March):395–421. <https://doi.org/10.1146/annurev-statistics-060116-054045>
- Saez M, Barceló MA (2022) Spatial prediction of air pollution levels using a hierarchical Bayesian spatiotemporal model in Catalonia, Spain. *Environ Model Softw* 151:105369. <https://doi.org/10.1016/j.envsoft.2022.105369>
- Simpson DP, Rue H, Martins TG, Riebler A, Sørbye SH (2017) Penalising model component complexity: a principled, practical approach to constructing priors (with discussion). *Stat Sci* 32(1):1–46. <https://doi.org/10.1214/16-STSS76>
- Tobias A, Royé D, Íñiguez C (2023) Heat-attributable mortality in the summer of 2022 in Spain. *Epidemiology* 34(2):e5–e6. <https://doi.org/10.1097/EDE.0000000000001583>
- Tobías A, Íñiguez C, Royé D (2023) From research to the development of an innovative application for monitoring heat-related mortality in Spain. *Environ Health* 1(6):416–419. <https://doi.org/10.1021/envhealth.3c00134>
- van Niekerk, Krainiski E, Rustand D, Rue H. A new avenue for Bayesian inference with INLA. *arXiv:2204.06797v1*, April 14, 2022. <https://doi.org/10.48550/arXiv.2204.06797>.
- Wannemuehler K, Lyles R, Waller L, Hoekstra R, Klein M, Tolbert P (2009) A conditional expectation approach for associating ambient air pollutant exposures with health outcomes. *Environmetrics* 20(7):877–894. <https://doi.org/10.1002/env.978>
- Wang XY, Guo Y, Fitzgerald G, Aitken P, Tippet V, Chen D, Wang X, Tong S (2015) The impacts of heatwaves on mortality differ with different study periods: a multi-city time series investigation. *PLoS ONE* 10:e0134233. <https://doi.org/10.1371/journal.pone.0134233>
- Watanabe S (2010) Asymptotic equivalence of Bayes cross validation and widely applicable information criterion in singular learning theory. *J Mach Learn Res* 11:3571–3594. <https://doi.org/10.5555/1756006.1953045>

World Health Organization. Heat and Health. 2025 [Available at: <https://www.who.int/news-room/fact-sheets/detail/climate-change-heat-and-health>. Accessed 5 June 2025]

Yin P, Chen R, Wang L, Liu C, Niu Y, Wang W, Jiang Y, Liu Y, Liu J, Qi J, You J, Zhou M, Kan H (2018) The added effects of heatwaves on cause-specific mortality: a nationwide analysis in 272 Chinese cities. *Environ Int* 121:898–905. <https://doi.org/10.1016/j.envint.2018.10.016>

Zhang L, Zhang Z, Ye T, Zhou M, Wang C, Yin P, Hou B (2018) Mortality effects of heat waves vary by age and area: a multi-area study in China. *Environ Health* 17:54. <https://doi.org/10.1186/s12940-018-0398-6>

Publisher's Note Springer Nature remains neutral with regard to jurisdictional claims in published maps and institutional affiliations.